Submitted to the
International Europhysics Conference on High Energy Physics
Aachen, Germany, July 17 - 23, 2003

Abstract: 507 **Sessions: HQCD,HP**

Inclusive jet production in neutral current deep inelastic scattering at HERA and parton dynamics at low x

ZEUS Collaboration

Abstract

Inclusive jet production in neutral current deep inelastic positron-proton scattering has been measured for boson virtualities $Q^2 > 25$ GeV^2. The data were taken at the HERA collider with centre-of-mass energy $\sqrt{s} = 300$ GeV using the ZEUS detector and correspond to an integrated luminosity of 38.7 pb^{-1}. Jets were identified using the longitudinally invariant k_T-cluster algorithm. Measurements of differential inclusive jet cross sections are presented as functions of jet transverse energy (E_T^{jet}), jet pseudorapidity (η^{jet}), Q^2 and Bjorken x with $E_T^{jet} > 6$ GeV and $-1 < \eta^{jet} < 3$. The data are compared to leading-logarithm parton-shower model predictions and next-to-leading-order QCD calculations using DGLAP evolution and parametrizations of the proton parton distribution functions. Special emphasis is given to the low E_T^{jet} forward-going (high η^{jet}) jets in order to search for deviations at low Q^2 and low x.

1 Introduction

The proton structure function F_2 can be calculated in perturbative QCD given an initial measurement via a set of renormalisation-group equations governing parton evolution. These evolution equations can be resummed in order to predict how cross sections for different processes change with Bjorken x (x_{Bj}) and photon virtuality (Q^2). One example of this resummation is the DGLAP equations [1], which have been tested and confirmed extensively at HERA and other high energy experiments. In another approach, the leading terms in $\ln(1/x)$ which appear in the evolution equations are resummed to yield the BFKL equation [2]. This QCD treatment of the parton evolution is expected to describe the HERA data better than DGLAP in the low x_{Bj} region of phase space. To test for the onset of BFKL evolution, measurements are needed in the lowest x_{Bj} (low parton momentum) regions of the HERA phase space.

This analysis explores the region where DGLAP parton evolution is not expected to be valid in order to investigate whether any deviations found might be better characterized by BFKL parton evolution. In the DGLAP formalism, the parton cascade that results in the hard scattering of the virtual photon with a parton in the proton is ordered in the parton virtuality. This ordering along the parton ladder implies an ordering in transverse energy of the partons, with the parton resulting from the hard scatter having the highest E_T. In the BFKL formalism the partons are emitted democratically in virtuality and E_T. Since the partons emitted at the bottom of the ladder are closest in space to the outgoing proton, they are manifested as forward jets. An excess of forward jets over the DGLAP prediction would provide an opportunity to test the applicability of BFKL evolution [3,4].

In this paper, measurements of differential cross sections for inclusive jet production in the laboratory frame of deep inelastic ep scattering are presented. The inclusive jet cross sections are measured as a function of jet transverse energy, jet pseudorapidity, Q^2 and x_{Bj}. The measurements are compared with leading-logarithm parton shower models and next-to-leading order (NLO) QCD predictions based on DGLAP evolution. The jet and kinematic cuts are designed to search for deviations at low Q^2 and low x_{Bj} where an excess of data over the DGLAP prediction could indicate an opportunity to test for BFKL evolution.

2 Theoretical Predictions

The data are compared to predictions from the Monte Carlo programs ARIADNE [5] and LEPTO [6], and to the NLO QCD calculations using the program DISENT [7]. The Monte Carlo models include approximations for higher-order effects in the QCD cascade.

However, the model dependence of these approximations can be large, and it is difficult to draw firm conclusions about possible deviations of the measured cross sections with respect to perturbative QCD predictions. ARIADNE models the QCD cascade with the color-dipole model, which treats gluons emitted from the quark-antiquark pairs as radiation from a color dipole between two partons. This causes the partons to not be ordered in transverse momentum, yielding a partonic final state more similar to that predicted by BFKL. The LEPTO Monte Carlo is based on first-order QCD matrix elements (like ARIADNE) plus parton showers modelled as in the DGLAP formalism. In both cases, fragmentation into hadrons was performed using the LUND [8] string model. Radiative corrections were computed with DJANGO v1.1 [9], which interfaces the LEPTO and ARIADNE Monte Carlo programs to HERACLES [10].

The DISENT calculation interfaces NLO matrix elements with parton density functions (PDF's) as calculated by CTEQ6 [11] to make parton level predictions of the cross sections. The number of flavors is set to 5; the $\overline{MS}$-scheme factorization and renormalisation scales are set to Q^2; $\alpha_s(M_Z)$ is set to 0.118. Comparison of the data with an NLO calculation is a more reliable test of QCD than comparison with Monte Carlo models since the higher order (NLO) process is treated analytically according to the rules of QCD. It has the drawback, however, of being a fixed-order calculation, and no attempt is made within the calculation at modeling the higher order corrections. The partonic cross sections are corrected for hadronization effects using ARIADNE.

In this paper, two different NLO calculations are used to compare to the data in two different phase space regions (defined below). Quark-parton model (i.e. single jet) events are expected to dominate the first region; therefore, the DISENT predictions for this region has LO = $\mathcal{O}(\alpha_s^0)$ and NLO = $\mathcal{O}(\alpha_s^1)$. The second phase space region is expected to be dominated by the contributions from boson-gluon fusion and QCD Compton processes, and the DISENT calculation has LO = $\mathcal{O}(\alpha_s^1)$ and NLO = $\mathcal{O}(\alpha_s^2)$. The uncertainty on the NLO calculations due to the absence of higher-order terms is estimated by increasing and decreasing the renormalisation scale by a factor of two. The uncertainty on the NLO calculations due to the experimental uncertainties of each data set used in the determination of the proton PDF's is calculated making use of the results of the CTEQ6 analysis.

3 Data Selection and Jet Search

This analysis is based on data collected in the 1996-1997 running period where the center-of-mass energy of the 820 GeV proton and 27.5 GeV positron beams was $\sqrt{s} \sim 300$ GeV and corresponds to an integrated luminosity of 38.7 ± 0.6 pb^{-1}. The ZEUS detector is described in detail elsewhere [12]. Neutral current deep inelastic scattering events were selected by requiring an isolated high-energy positron ($E'_e > 10$ GeV) in the final state, and cuts were applied using the uranium-scintillator calorimeter and central tracking detectors in order to reject cosmic and charged current events and beam-gas background. A cut on the $E - p_z$ of the event was made to reject photoproduction and radiative events. The reconstruction of the kinematic variables used the angles of the scattered electron and the hadronic system [13]. The hadronic angle γ_h, which corresponds to the direction of the outgoing quark in quark-parton model events, was reconstructed with the calorimeter measurement of the hadronic final state.

The jet search was performed on all calorimeter cells, excluding those belonging to the scattered positron. Jets with transverse energy $E_{T,jet} > 6$ GeV and pseudorapidity $-1 < \eta_{jet} < 3$ were selected in the $\eta - \phi$ plane of the laboratory frame with the longitudinally-invariant k_T-cluster algorithm [14] in the inclusive mode [15], which groups cells (or particles) according to their relative momenta into jets. The jet cross sections are measured as functions of jet transverse energy $E_{T,jet}$ and pseudorapidity η_{jet}, and in kinematic variables Q^2 and x_{Bj}. All data cross sections are corrected for detector acceptance with ARIADNE, which is also used to calculate QED radiative effects.

Only events with $Q^2 > 25$ GeV^2 and $y > 0.04$ are considered in the measurement. The analysis is performed twice: once in the full phase space given by the aforementioned kinematic restrictions, and once with the requirements that the hadronic angle be found in the rear part of the detector ($\cos\gamma_h < 0$) and the jet(s) be found in the forward part of the detector ($\eta_{jet} > 0$). The hadronic angle restriction is made in order to reject single-jet events from the sample where the hadronic angle is aligned with an outgoing quark in the forward direction (quark-parton model events). This cut has the advantage of enhancing the dijet or multijet contribution, while not restricting the phase space of the current jet, i.e. the jet at the top of the parton cascade closest to the hard interaction. Henceforth, we will use the terminology 'inclusive phase space' and 'dijet phase space' to describe these two kinematic regions.

4 Results

The differential inclusive jet cross sections in η_{jet} and $E_{T,jet}$ for the inclusive phase space are shown in Figures 1 and 2, respectively. Because these jet cross sections are measured inclusively, each jet contributes to the cross section and thus multijet events contribute more than single-jet events. In the entire sample considered, 400,101 of the total 454,092 events are classified as single-jet events, yielding a contribution from dijets and multijets of 12%. A study of the sources contributing to the systematic uncertainties (shown as the thinner of the two error bars in the figures) revealed the dominant uncertainty to be that due to the uncertainty in the acceptance correction. The systematic error bars do not include a 1.6% uncertainty in the luminosity measurement. The uncertainty due to the absolute energy scale of the jets ($\pm 3\%$) is shown separately as a shaded band in each figure. The leading order Monte Carlo models can reproduce the shape and normalisation of the data, but the relative difference between data and NLO calculation grows rapidly in the forward region (high η_{jet}). For the cross section measured in $E_{T,jet}$, the data are about $20 - 25\%$ above the NLO in the lowest $E_{T,jet}$ bins, and then approach the NLO calculation at higher $E_{T,jet}$. The measured $d\sigma/dE_{T,jet}$ drops by 5 orders of magnitude in the $E_{T,jet}$ range considered.

Cross sections in x_{Bj} and Q^2 for events with one or more jets are given in Figures 3 and 4, respectively. The NLO calculation can describe the data well except in the lowest bins of Q^2 and x_{Bj}. The cross section in x_{Bj} turns over in the lowest x_{Bj} bins due to the lower cutoff in Q^2.

In order to reduce the contribution of quark-parton model events, the same cross sections are shown in Figures 5-8 with the restrictions on the hadronic angle of the event and jet pseudorapidity. The renormalization uncertainty is significantly larger for the dijet phase space than for the inclusive phase space. For the dijet phase space, the data and the NLO calculation agree within the renormalization-scale uncertainty for all variables.

5 Conclusion

Measurements of differential cross sections in $E_{T,jet}$, η_{jet}, Q^2 and x_{Bj} for inclusive jet production in neutral current deep inelastic scattering have been presented using 38.7 pb^{-1} of ZEUS data. The low x_{Bj} region has been probed for events with $Q^2 > 25$ GeV^2 and at least one jet with 6 GeV of transverse energy. Two phase space regions have been studied: one inclusive region and one with an additional requirement on the hadronic angle of the event ($\cos\gamma_h < 0$) and a more limited window of jet pseudorapidity ($\eta_{jet} > 0$); the restrictions imposed on the second phase space region enhance the dijet and multijet contributions while not restricting the transverse energy of the current jet.

The leading-logarithm parton shower calculations can describe the shape of the data in most variables, but the color-dipole model generally gives a better description of both the data shape and normalization. An large excess of the data over the NLO is observed in the jet cross section for the inclusive phase space at high jet η and low x_{Bj}. This excess is reduced considerably in the dijet phase space where the cross section is dominated by boson-gluon fusion events, but the theoretical uncertainty increases significantly. Accordingly, the present theoretical limitations prevent establishing an environment suitable for decisive tests of BFKL dynamics in these data. Improved calculations, perhaps using the BFKL approach, are needed to give a more accurate prediction in this region.

References

[1] V.N. Gribov and L.N. Lipatov, Sov. J. Nucl. Phys. **15**, 438 (1972);
L.N. Lipatov, Sov. J. Nucl. Phys. **20**, 94 (1975);
Yu.L. Dokshitzer, Sov. Phys. JETP **46**, 641 (1977);
G. Altarelli and G. Parisi, Nucl. Phys. **B 126**, 298 (1977).

[2] E.A. Kuraev, L.N. Lipatov, V.S. Fadin, Sov. Phys. JETP **45**, 199 (1977);
Ya.Ya. Balitskiĭ and L.N. Lipatov, Sov. J. Nucl. Phys. **28**, 822 (1978).

[3] A.H. Mueller, Nucl. Phys. Proc. Suppl. **C 18**, 125 (1991);
A.H. Mueller, J. Phys. **G 17**, 1443 (1991).

[4] J. Bartels, A. De Roeck, M. Loewe, Z. Phys. **C 54**, 645 (1992);
J. Kwiecinski, A.D. Martin, P.J. Sutton, Phys. Lett. **B 287**, 254 (1992);
W.K. Tang, Phys. Lett. **B 278**, 363 (1992).

[5] L. Lönnblad, Comp. Phys. Comm. **71**, 15 (1992);
L. Lönnblad, Z. Phys. **C 65**, 285 (1995).

[6] G. Ingelman, A. Edin and J. Rathsman, Comp. Phys. Comm. **101**, 108 (1997).

[7] S. Catani and M.H. Seymour, Nucl. Phys. **B 485**, 291 (1997). Erratum in Nucl. Phys. **B 510**, 503 (1998).

[8] B. Andersson et al., Phys. Rep. **97**, 31 (1983).

[9] K. Charchula, G.A. Schuler and H. Spiesberger, Comp. Phys. Comm. **81**, 381 (1994);
H. Spiesberger, HERACLES *and* DJANGOH*: Event Generation for ep Interactions at HERA Including Radiative Processes*, 1998, available on `http://www.desy.de/~hspiesb/djangoh.html`.

[10] A. Kwiatkowski, H. Spiesberger and H.-J. Möhring, Comp. Phys. Comm. **69**, 155 (1992). Also in *Proc. Workshop Physics at HERA*, 1991, DESY, Hamburg.

[11] J. Pumplin et al., JHEP **0207**, 012 (2002).

[12] ZEUS Coll., U. Holm (ed.), *The ZEUS Detector*. Status Report (unpublished), DESY (1993), available on `http://www-zeus.desy.de/bluebook/bluebook.html`.

[13] S. Bentvelsen, J. Engelen and P. Kooijman, *Proc. Workshop on Physics at HERA*, W. Buchmüller and G. Ingelman (eds.), Vol. 1, p. 23. Hamburg, Germany, DESY (1992).

[14] S. Catani et al., Nucl. Phys. **B 406**, 187 (1993).

[15] S.D. Ellis and D.E. Soper, Phys. Rev. **D 48**, 3160 (1993).

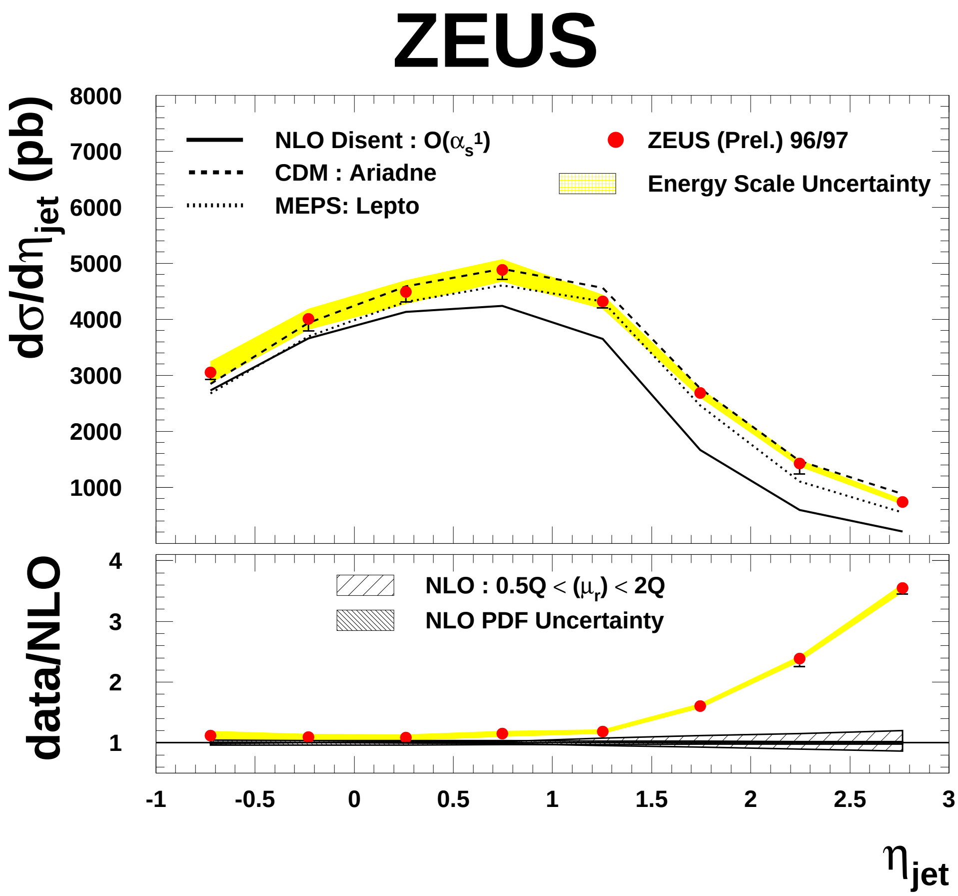

Figure 1: *a) Measured differential inclusive jet cross section $d\sigma/d\eta_{jet}$ for the inclusive phase space. Ariadne (CDM) prediction given by the dashed line; Lepto (MEPS) prediction given by the dotted line. The bold vertical error bars represent the statistical uncertainties of the data, the thinner error bars show systematic uncertainties added in quadrature, except for that associated with the uncertainty in the absolute energy scale of the jets (shaded band). b) Relative difference of the measured inclusive jet cross-section $d\sigma/d\eta_{jet}$ to the NLO DISENT calculation with renormalisation scale $\mu_R^2 = Q^2$ The widely spaced hatched band shows the renormalization scale uncertainty of the calculation. The thinly spaced hatched band shows the PDF uncertainty.*

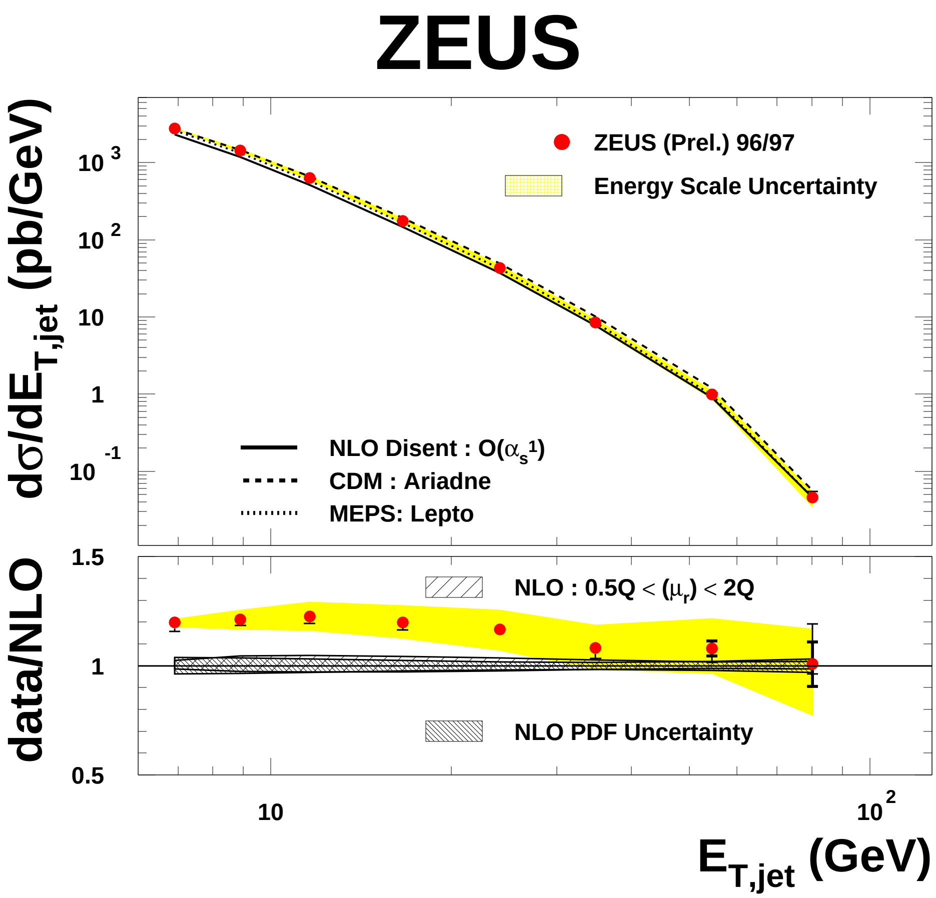

Figure 2: *Measured differential inclusive jet cross section $d\sigma/dE_{T,jet}$ for the inclusive phase space. Other details as in the caption to Fig. 1.*

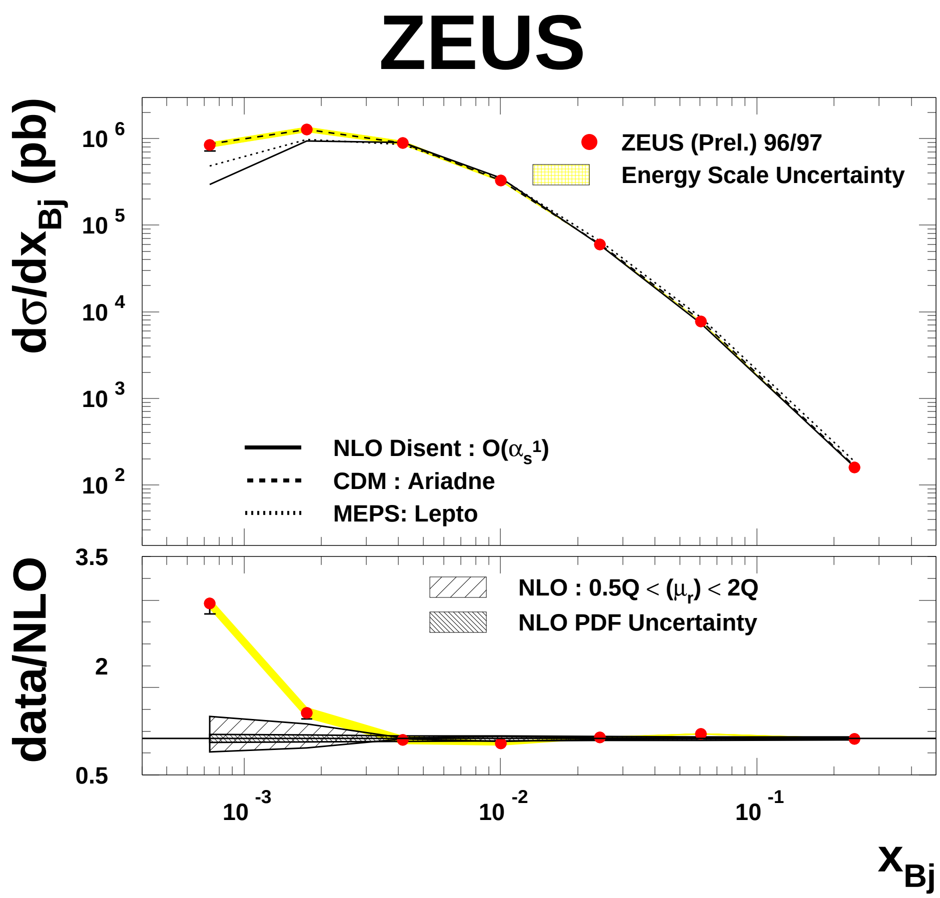

Figure 3: *Measured differential cross section $d\sigma/dx_{Bj}$ for events with one or more jets in the inclusive phase space. Other details as in the caption to Fig. 1.*

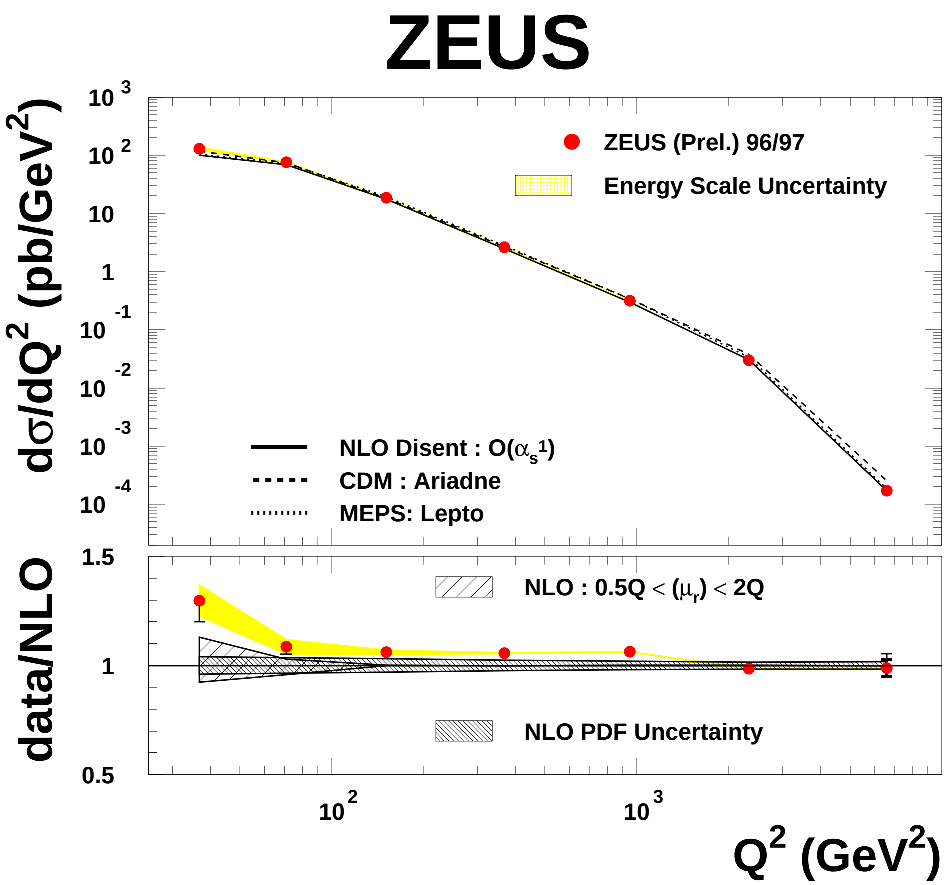

Figure 4: *Measured differential cross section $d\sigma/dQ^2$ for events with one or more jets in the inclusive phase space. Other details as in the caption to Fig. 1.*

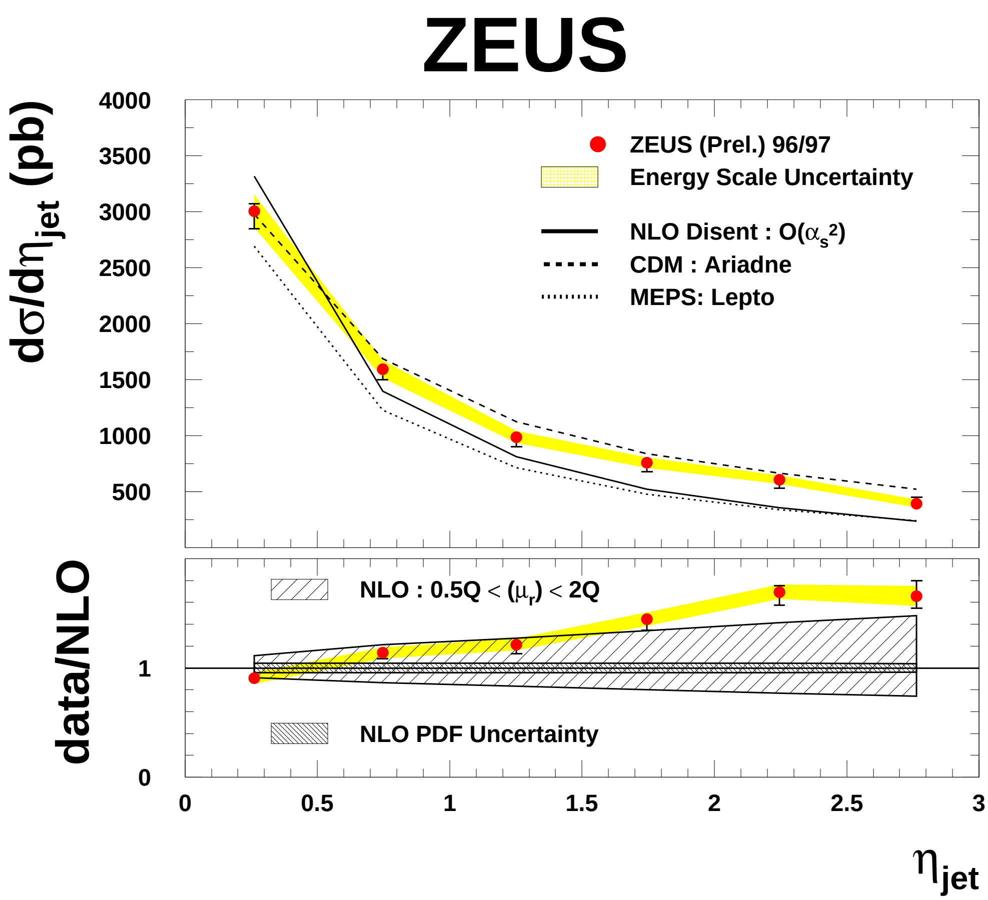

Figure 5: *a) Measured differential inclusive jet cross section $d\sigma/d\eta_{jet}$ for the dijet phase space. Ariadne (CDM) prediction given by the dashed line; Lepto (MEPS) prediction given by the dotted line. The bold vertical error bars represent the statistical uncertainties of the data, the thinner error bars show systematic uncertainties added in quadrature, except for that associated with the uncertainty in the absolute energy scale of the jets (shaded band). b) Relative difference of the measured inclusive jet cross-section $d\sigma/d\eta_{jet}$ to the NLO DISENT calculation with renormalisation scale $\mu_R^2 = Q^2$ The widely spaced hatched band shows the renormalization scale uncertainty of the calculation. The thinly spaced hatched band shows the PDF uncertainty.*

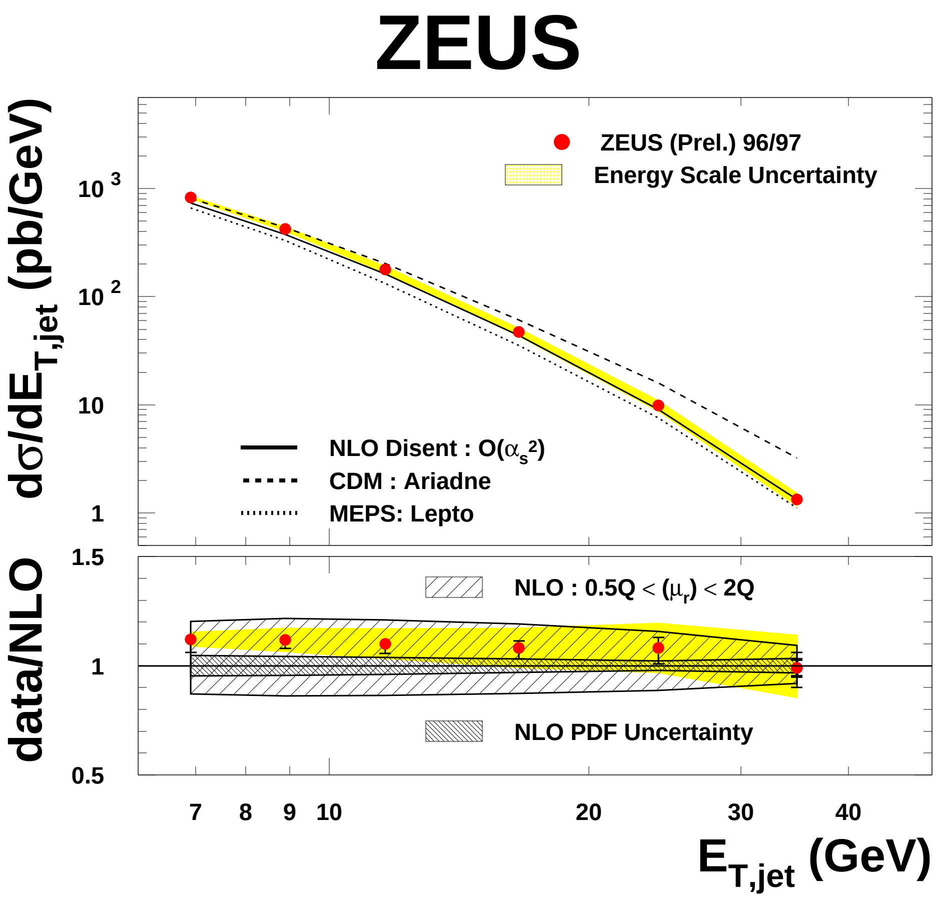

Figure 6: *Measured differential inclusive jet cross section $d\sigma/dE_{T,jet}$ for the dijet phase space. Other details as in the caption to Fig. 5.*

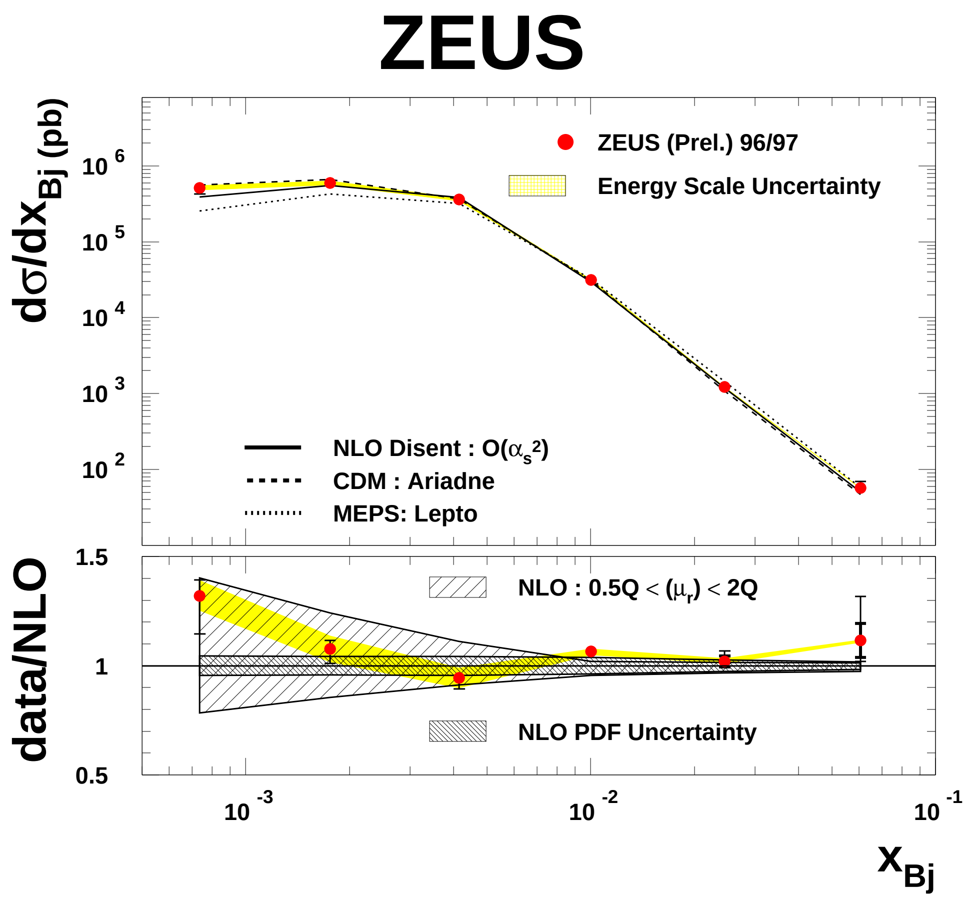

Figure 7: *Measured differential cross section $d\sigma/dx_{Bj}$ for events with one or more jets in the dijet phase space. Other details as in the caption to Fig. 5.*

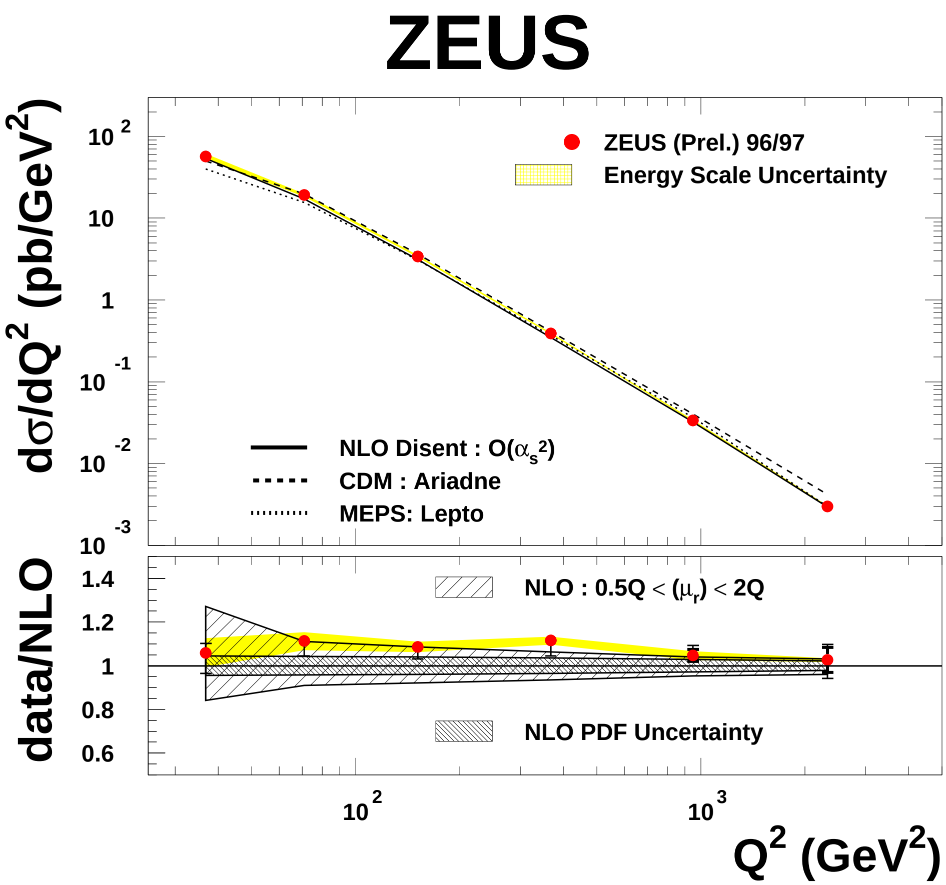

Figure 8: *Measured differential cross section $d\sigma/dQ^2$ for events with one or more jets in the dijet phase space. Other details as in the caption to Fig. 5.*